

Effect of Zinc Industrial waste on the Mechanical and microstructural properties of the Ternary Blended Concrete

Tarunkumar Pandiyan¹, Elavenil Solaiyan^{2*}

¹ Research Scholar, School of Civil Engineering, Vellore Institute of Technology.

² Professor, School of Civil Engineering, Vellore Institute of Technology.

* Corresponding author

E-Mail: elavenil.s@vit.ac.in, Tel: 9840237492



19

20 **ABSTRACT**

21 The rapid growth of infrastructure leads to industrial waste accumulation and natural resource depletion,
22 raising the need for sustainable solutions. When zinc is refined, a significant amount of non-
23 biodegradable material called jarosite (JS) is generated, requiring proper environmentally friendly
24 disposal techniques. The present study investigates ternary blended of portland cement with partial
25 replacement of 20% ground granulated blast furnace slag and jarosite at (5 – 25%) as a binder material
26 to develop a sustainable concrete mix. To comprehend the effectiveness of jarosite-GGBS blends in
27 concrete, experimental research is performed to investigate the mechanical properties of ternary blended
28 concrete. Additionally, SEM and XRD analysis were used to observe the microstructure and chemical

phases of the developed concrete. From the experimental investigations, it is perceived that the incorporation of jarosite-GGBS blended concrete increased strength properties for all the mix proportions. The microstructure study shows a decrease in voids and the formation of sufficient CSH gel, justifying improved mechanical properties. The maximum increase in compressive strength of 50.93% is observed with 10% jarosite and 20% GGBS in the concrete mix. The overall research findings provide insight into the functionality of GGBS and jarosite blended concrete and the potential of jarosite as a sustainable, reusable industrial waste material.

Keywords: Jarosite; Industrial waste; Sustainable waste management; Concrete.

1. Introduction

Concrete is a vital building component that strongly influences the development of a growing infrastructure. Nevertheless, an abundance of natural resources must be utilized in its production (Wang et al. 2023). The worldwide demand for concrete is projected to surpass about 18 million tonnes annually by 2050 (Rakesh Kumar Reddy et al. 2023). The approximate carbon dioxide emission per tonne of cement generated varied between 0.7 to 1.1 tonnes (Rashad 2015). Based on the United Nations framework for tackling the effects of climate change, various countries including India have ratified the Paris Agreement, with the primary objective being to restrict the rise in the average global temperature to 1.5 °C by the incorporation of alternate concrete materials in the form of industrial by-products (Delbeke et al. 2019).

Cement production (an energy-intensive process) has increased drastically over the past decade to meet the construction industry's ever-increasing demand. Studies (Zhaurova et al. 2021) have disclosed that the cement industry on its own emits around 5% of the total CO₂ produced worldwide, and it is anticipated that this percentage will ascend to 8% in the coming years (Khaiyum et al. 2023). Multiple research

studies are currently being carried out on supplemental cementitious materials(SCM) to replace cement(Gupta and Chaudhary 2022). It is anticipated that this will reverse its atmospheric emission content (Khotbehsara et al. 2015; Koushkbaghi et al. 2019). Such replacement materials like SCM can be discovered as the end products of various industries. Nevertheless, India generates nearly 960 million tonnes of solid waste per year(Sharma et al. 2018). Due to the enormous production of waste material, landfill management is becoming more expensive, and the environment is becoming more toxic. To confront its development in a land fill for waste material, this urges suitable treatment and alternative solutions for sustainable disposal (Pappu et al. 2007). Waste from agriculture(Thirukumaran et al. 2023), domestic waste(Paramasivan et al. 2023), Solid wastes from thermal power plants (fly ash(Naveen Arasu et al. 2023)), the steel and iron industry(Ground granulated blast furnace slag), Aluminium industrial waste (red mud), zinc industrial waste (jarosite), and the cement industry waste (cement kiln dust)(Siddique 2014) are utilized in the concrete as cementitious material as a safe sustainable disposal of these by-products Instead of landfill.

2. Literature review

The toxic waste widely recognized as jarosite is generated by the zinc industry. The process of roasting rich zinc ore to 900°C and then leaching it with the assistance of a hot acid to create jarosite. Almost every developed and developing nation generates jarosite. European Union produces 0.60 million tonnes of hazardous zinc residue each year (Asokan et al. 2010; Pappu et al. 2006). The Ministry of Environment and Forests' Schedule II asserted in 2008 that the material's toxicity was hazardous based on the presence of heavy metals like copper, zinc, lead, chromium, and cadmium present in raw jarosite. Furthermore, it has also been classified as a very hazardous material by the European Union and the Basel Convention(Agrawal et al. 2004). Various attempts have been made to utilize this zinc industry waste in the last decade. The toxicity of jarosite can be reduced by mixing lime, which stabilizes the heavy metal content (Gupta and Prasad 2018a). Gupta et al. evaluated cement jarosite lime blends in the lab for

strength using measures like split tensile strength and unconfined compressive strength at varying curing times of 7, 28, and 90 days this study's results indicated that as the lime content and curing time increased, the strength increased respectively. Further in the study (Gupta and Prasad 2018b), the authors used lime-treated jarosite to test its strength by measuring the unconfined compressive strength and split tensile strength of jarosite stabilised by Ground granulated blast furnace slag (GGBS) and lime blends, the authors have investigated the impact of blast-furnace slag, lime, and curing time in the jarosite stabilisation and geotechnical applications, and determined that strengths increase nonlinearly as GGBS, lime, and curing time increases. Katsioti et al. explored the possibility of substituting natural gypsum with jarosite/alunite precipitate when manufacturing clinker. To conduct the test, gypsum was replaced to varying degrees with jarosite, and their compressive strength, setting time, water-soluble chromium content, and grindability were all evaluated. According to the study, a larger substitution of jarosite chemical for gypsum leads to a shorter setting time as well as lower compressive strength values(Katsioti et al. 2005).

Some authors have examined the jarosite-added concrete. Mehra et al. used fly ash instead of cement and jarosite for fine aggregates. A laboratory investigation was carried out to evaluate the durability and mechanical properties. Furthermore, three distinct water-to-cement ratios were used for the microstructural analysis. They discovered that the concrete with jarosite demonstrates acceptable mechanical and durability qualities, further supported by XRD testing and SEM pictures. Additionally, the findings suggested that concrete containing 15% jarosite might be appropriate for use in road construction.(Mehra et al. 2018; Mehra et al. 2016a; Mehra et al. 2016b). Gupta et al. encountered that as the lime concentration increased, the unconfined compressive strength and split tensile strength of the lime-treated jarosite increased polynomially (Gupta and Prasad 2018c) Mymrin et al. studied that materials treated with jarosite could be made stronger by adding a slight amount of lime or Portland cement (Mymrin A et al. 2005; V.mymrin and Vaamonde 1999).

100 **2. Research Significance**

101 Investigation on the partial substitution of jarosite for cement in concrete mixtures along with other
102 industrial waste is scarce. Furthermore, a thorough investigation of the impact of jarosite as a partial
103 cement substitution in the chemical phase matrix of concrete is still concerning. Correspondingly, an
104 attempt has been made to investigate the mechanical and microstructure behavior of concrete mixes using
105 jarosite-GGBS-OPC blends in the current study. This study may contribute to the limited research on
106 using jarosite in concrete mixtures as a cementitious material.

107 **3. Material and methods**

108 The zinc industrial waste by-product (Jarosite) used in this research was collected from Hindustan Zinc
109 Ltd, located at Udaipur, Rajasthan. The jarosite waste was sundried at the industrial yard for 24 hours
110 and stored in a water-resistant bag at a dry place. The collected jarosite is yellowish in colour, as
111 represented in Figure 1. As per ASTM C618 standards, jarosite can be determined as a pozzolanic
112 material though the calcium oxide content is less than 2%, materials like GGBS can be blended to form
113 a supplemental cementitious material. Table 1 provides the chemical and physical characteristics of
114 Ordinary Portland cement (OPC) Jarosite (JS) and ground granulated blast furnace slag (GGBS). The
115 Chemical composition of jarosite is 27.86% Al_2O_3 , as per Bumanis et al. Al_2O_3 plays a vital role in
116 pozzolanic activities with a higher surface area of $85.320 \text{ (m}^2\text{/g)}$, it can be used as supplementary
117 cementitious material (Bumanis et al. 2020). Figure 2 represents the particle size distribution of the
118 binding material, stating that the fineness of jarosite is much lower than that of ordinary Portland cement,
119 which helps to reduce the fine voids in the concrete matrix. OPC 53 grade is the primary binding agent
120 in this study according to IS: 12269. M-sand size of 4.75mm and coarse aggregate of size 12mm are used
121 in this study. OPC, M-sand, and coarse aggregate are procured from the local vendor, confirming to IS:
122 456(2000).

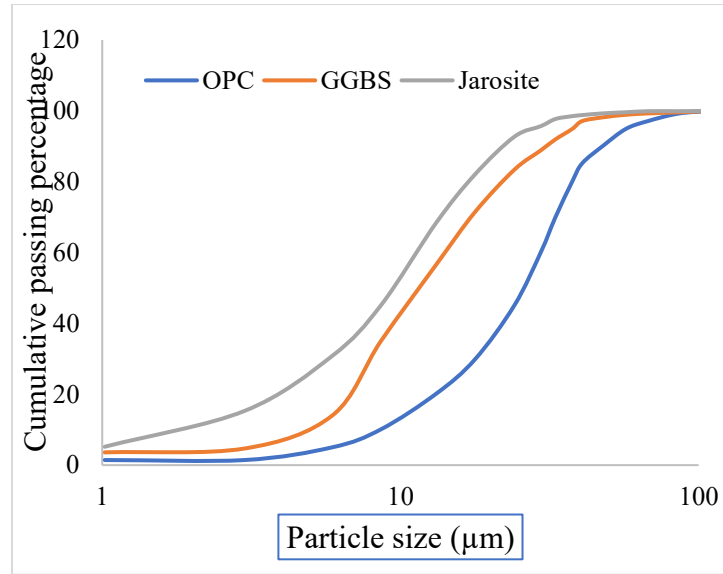
123 **Table 1.** Chemical and physical characteristics of OPC-53, jarosite(JS), and Ground granulated blast
 124 furnace slag (GGBS).

Formula	OPC-53	Jarosite	GGBS
Al ₂ O ₃ (%)	4.40	27.86	18.33
CaO (%)	66.45	1.54	32.98
Fe ₂ O ₃ (%)	4.86	4.27	0.82
K ₂ O (%)	0.45	1.78	-
MgO (%)	0.88	0.53	8.88
Na ₂ O (%)	0.10	0.32	-
SiO ₂ (%)	19.01	55.13	35.08
SO ₃ (%)	2.81	-	2.99
ZnO (%)	-	-	-
PbO (%)	-	-	-
TiO ₂ (%)	-	1.80	-
P ₂ O ₅ (%)	-	0.19	-
Specific gravity	3.15	2.88	2.85
Specific surface area (m ² /g)	3.264	85.350	4.245



(a)

(b)

Figure 1. Industrial waste (a)-Jarosite (b)- Ground granulated blast furnace slag**Figure 2** – Particle size distribution of the binding materials

4. Experimental procedure

4.1 Mechanical Analysis

In order to perform the compression test, the specimens were positioned within the compression testing machine (CTM). The load was incrementally applied to the specimen until it reached its breaking point. The mechanical property test was conducted on 7, 14, and 28 days of curing. A total of one hundred and sixty-two specimens were cast, which include cubes, prisms, and cylinders leaving three samples for each test and taking the average strength value for further analysis. The tests have been carried out in compliance with the provisions of the IS: 516(BIS 1959) code. Figure 3 represents the compressive strength testing of cubes, tensile strength testing of cylinders, and flexural strength testing of prism.



(a)

(b)

(c)

Figure 3. (a) compressive strength testing (b) tensile strength testing (c) flexural strength testing.

4.2 Microstructural Analysis

Scanning electron microscopy (SEM) and x-ray diffraction (XRD) analysis have been performed for microstructure study. After 28 days, curing specimens are tested for mechanical properties. The tested specimens were powdered into 75 μ mesh size particles to conduct the XRD study. Correspondingly, thin concrete flakes from the crushed concrete specimens are collected for investigation under a scanning electron microscope.

5. Mix design and proportioning

In this research work, the M30 grade of concrete with a targeted mean compressive strength of 38.25 N/mm² was designed in accordance with IS:10262-2019. The Ground granulated blast furnace slag (GGBS) are replaced with 20% of this percentage of GGBS replacement based on the study conducted by authors adek et al. (Ainie Mat Dom et al. 2022), and yamgar et al. (Sunil Bhagwan Yamgar and S.R.Takkalaki 2018) of the weight of cement (OPC), along with Jarosite replacement ranging from 0% to 25% of the weight of cement. The water-cement ratio was maintained at 0.45 throughout various mix ratios. Detailed proportions of the concrete specimens for each mix are shown in Table 2. In accordance with IS: 516-1959 and Table 1 of IS: 10086-1982, multiple testing specimens were cast, as represented

158 in Table 3. A total of six specimens of each mix were made for each of the necessary experiments for
 159 assessing the concrete's mechanical strength.

160 **Table 2.** Concrete mix proportions.

S.No	Mix	Proportions	C	G	J	FA	CA	Water	Water/ Cement ratio
		Ratios	(Kg)	(20%) (Kg)	(5-25%) (Kg)	(Kg)	(Kg)	(Kg)	
1	M1	100%C	8.69	0	0	12.47	22.91	3.476	0.45
2	M2	75%C+ 20%G+ 5%JS	6.517	1.738	0.435	12.47	22.91	3.476	0.45
3	M3	70%C+ 20%G+ 10%J	6.083	1.738	0.869	12.47	22.91	3.476	0.45
4	M4	65%C+ 20%G+ 15%J	5.652	1.738	1.3	12.47	22.91	3.476	0.45
5	M5	60%C+ 20%G+ 20%J	5.214	1.738	1.738	12.47	22.91	3.476	0.45
6	M6	55%C+ 20%G+ 25%J	4.779	1.738	2.173	12.47	22.91	3.476	0.45

161 C-Ordinary Portland Cement, G- Ground granulated blast furnace slag, J- Jarosite, FA- Fine Aggregate, CA- Coarse Aggregate.

162 **Table 3.** Detailed specifications of the concrete specimens

Specimen types	Test	Size(mm)	Number of specimens
Concrete cubes	Compressive strength	100 x 100 x 100	6 x 9 = 54
Concrete Prism	Flexural strength	500 x 100 x 100	6 x 9 = 54
Concrete Cylinders	Split tensile strength	200 x 100	6 x 9 = 54

6. Result and discussion

6.1 Compressive Strength

The compressive strength of the mix for 7, 14, and 28 days are represented in Figure 4. As indicated, At 28 days of curing, the M3 mix with a 10% jarosite and 20% ground granulated blast furnace slag shows a maximum increase of 50.93% in compressive strength with respect to controlled mix M1 with 100% ordinary portland cement. As the jarosite percentage increased above the 10% replacement level, the compressive strength gradually decreased to 2.67% at a 25 percentage replacement. With the incorporation of jarosite and GGBS, The 5% jarosite replacement mix showed a decrease in initial strength of 10.86%. This is due to the lack of pozzolanic materials from (10-25%) replacement levels an increase in initial strength is observed with the highest increment at M3 mix. The 14-day cured concrete specimens show similar strength patterns as the 7-day cured specimens with an M3 mix ratio of 35.46% increment in the compressive strength compared to the controlled M1 mix. The M2 and M6 mix ratios provided an 8% decrement in the compressive strength at 14 days this is due to a lack of pozzolanic materials. The jarosite and GGBS blended concrete provides improvement in strength due to the dense concrete structure formed by jarosite and its fineness that fills the voids between the cement elements(Ray et al. 2020) while GGBS provides the additional SiO_2 and CaO together with additional Al_2O_3 supplemented in higher pozzolanic reaction showing additional strength capabilities. The compressive strength of the concrete specimens is maintained above the design strength of 30MPa as the jarosite replacement percentage is increased.

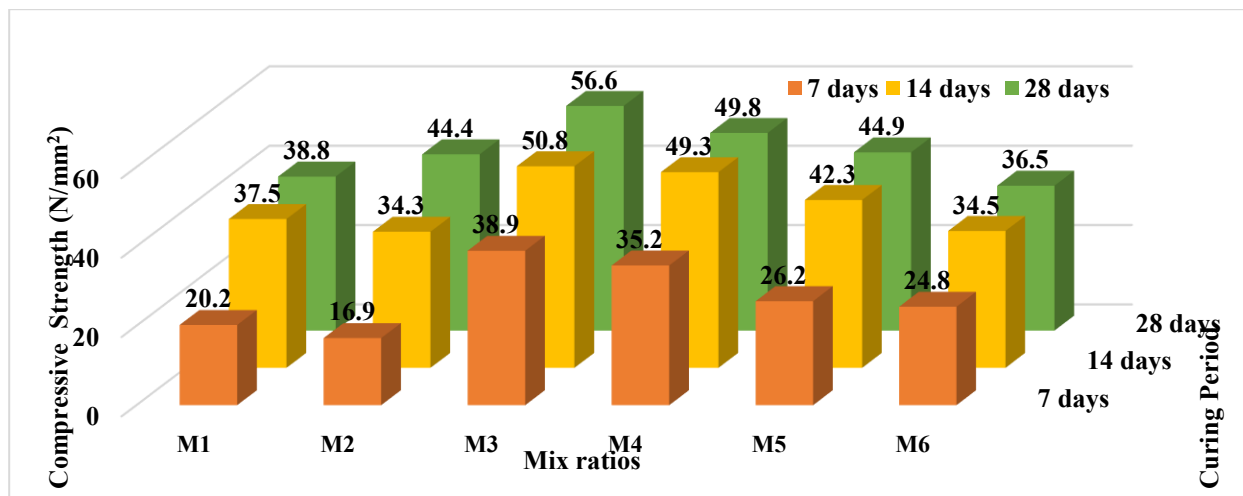
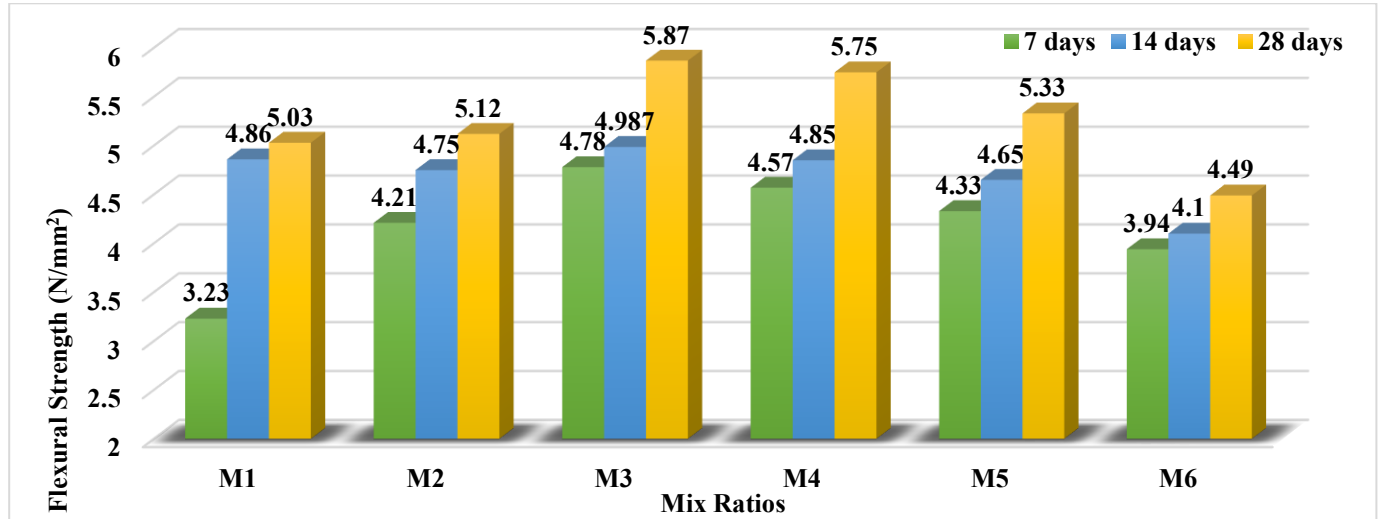


Figure 4 – Compressive strength results for 7,14,28 days of curing.

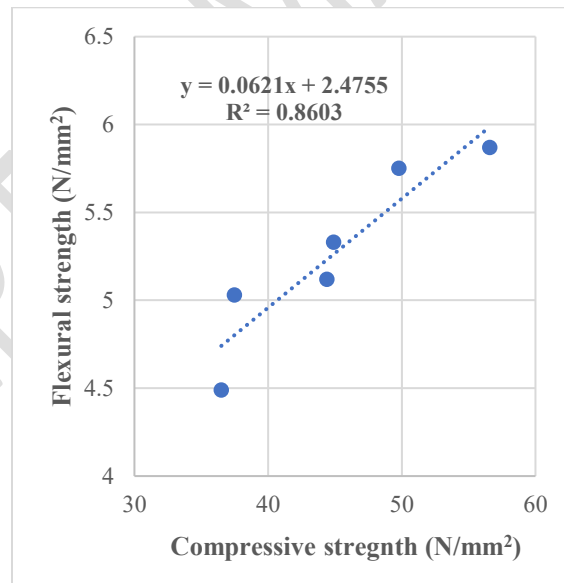
6.2 Flexural Strength

The correlation involving flexural strength and the curing period of JS and GGBS blended concrete has been illustrated in Figure 5. The findings reveal a positive correlation between the specimens' age and flexural strength, as well as the compressive strength of the concrete. It shows a 1.79, 16.7, 14.31, and 5.96% increase in flexural strength up to M5 mix ratios, whereas the M6 mix with a 25 % replacement level with jarosite provides a 10.74 % decrease in flexural strength. After seven days of curing, the percentage of increase in flexural strength are 30.34, 47.98, 41.48, 34.06, and 21.98 % with respect to the mix ratios, which is high compared to 28 days and 14 days of test analysis. This outcome coincides with the compressive strength analysis in which there is an improved initial strength with the addition of jarosite in concrete. A similar pattern of increase in flexural strength was observed (Kumar et al. 2016; Mehra et al. 2018). Nevertheless, in the previous studies, the maximum flexural strength was achieved at 20% and 25% replacement levels of jarosite due to various mix combinations. In this research, the maximum flexural strength is obtained at 10% replacement of OPC with jarosite at 5.87 Mpa with a 16.7% increase in flexural strength. Figure 6 depicts the correlation between the flexural and compressive strength of the developed concrete with linear regression equation, as represented by the R^2 value of

199 0.8603, which is greater than zero and closer to one resulting that the flexural strength of concrete is
 200 dependable on the compressive strength of concrete and can be predicted using the linear regression
 201 equation is certain accuracy.



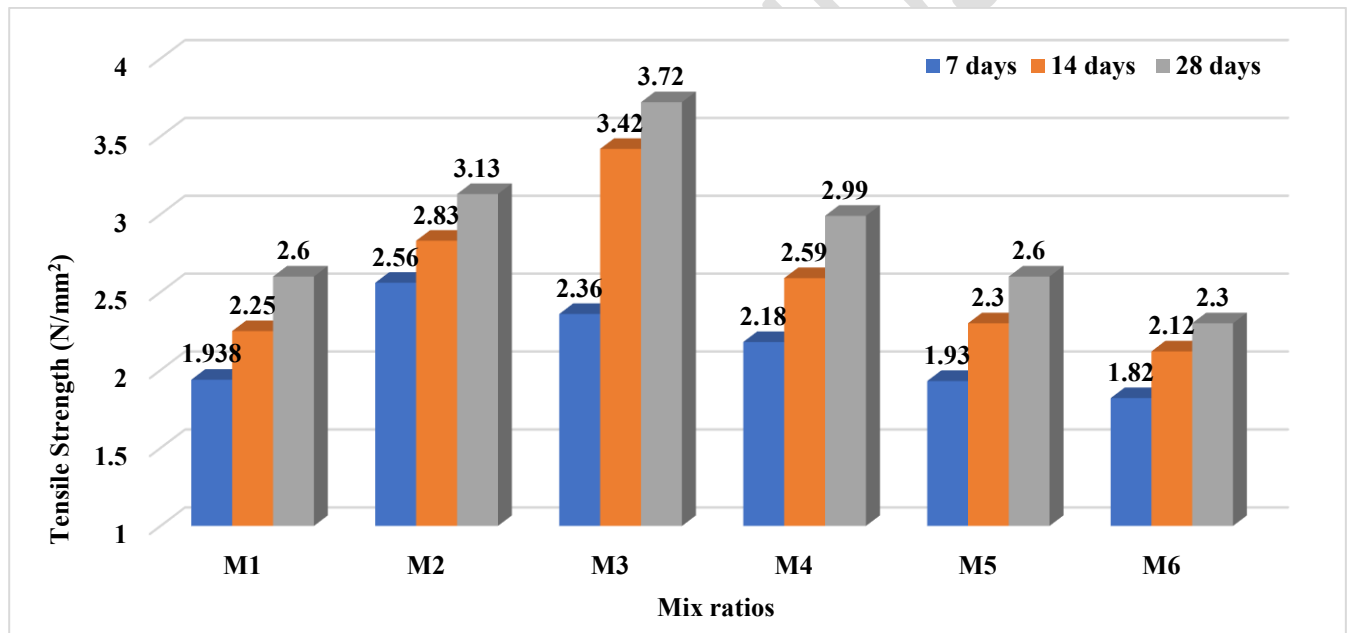
203 **Figure 5.** Flexural strength results for 7,14, and 28 days of curing.



205 **Figure 6.** Correlation between compressive and flexural strength of concrete

206 6.3 Tensile Strength

207 The relationship involving the split tensile strength of different specimens with the progressive insertion
 208 of jarosite in concrete is shown in Figure 7. There is a 20.4, 43.07, and 15% increment in tensile strength
 209 at 5, 10, and 15% increment in the 28 days of curing at 20% incorporation of jarosite. The 20% does not
 210 improve or decrease the split tensile strength, but there is an 11.54% decrease in strength with 25%
 211 addition of jarosite with the concrete. Figure 8 demonstrates the correlation between the tensile strength
 212 and compressive strength of the Jarosite GGBS blended concrete with linear regression equation as
 213 presented the R^2 value is 0.8098 hence it is closer to one the relation between tensile and compressive
 214 strength is related. That is, a change in compressive strength will change the tensile strength of the
 215 concrete.



216
 217 **Figure 7.** Tensile strength results for 7,14, and 28 days of curing.

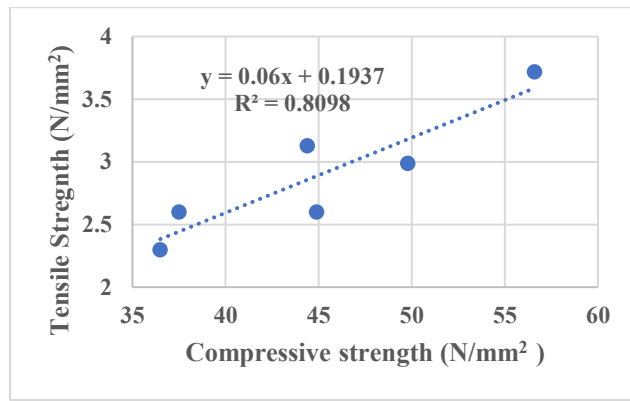


Figure 8. Correlation between Tensile strength and Compressive strength of concrete.

7. X-ray Diffraction Analysis

The X-ray diffraction patterns of the concrete mix after 28 days of curing are represented in Figure 7. The XRD analysis shows the crystalline phases of calcium silicates such as C_2S and C_3S , portlandite ($Ca(OH)_2$), and ettringite. Compared to the conventional M1 mix, the calcium silicate peaks are higher at M2 to M5. Similar XRD patterns are observed in (Saini et al. 2022b; Saini et al. 2022a). The Pattern of M3 has the highest peak at 26.78° , representing the formation of Calcium silicates that justifies the increase in strength properties of concrete. Similarly, at 53.63° , the unreacted portlandite tends to have the highest peak at M6 ratio, indicating that the volume of jarosite interacts with the hydration process, leading to a decrease in calcite peaks of M6. The SEM images of the M3 mix show high CSH and CH formation and Reduced ettringite formation that is justified in the XRD patterns.

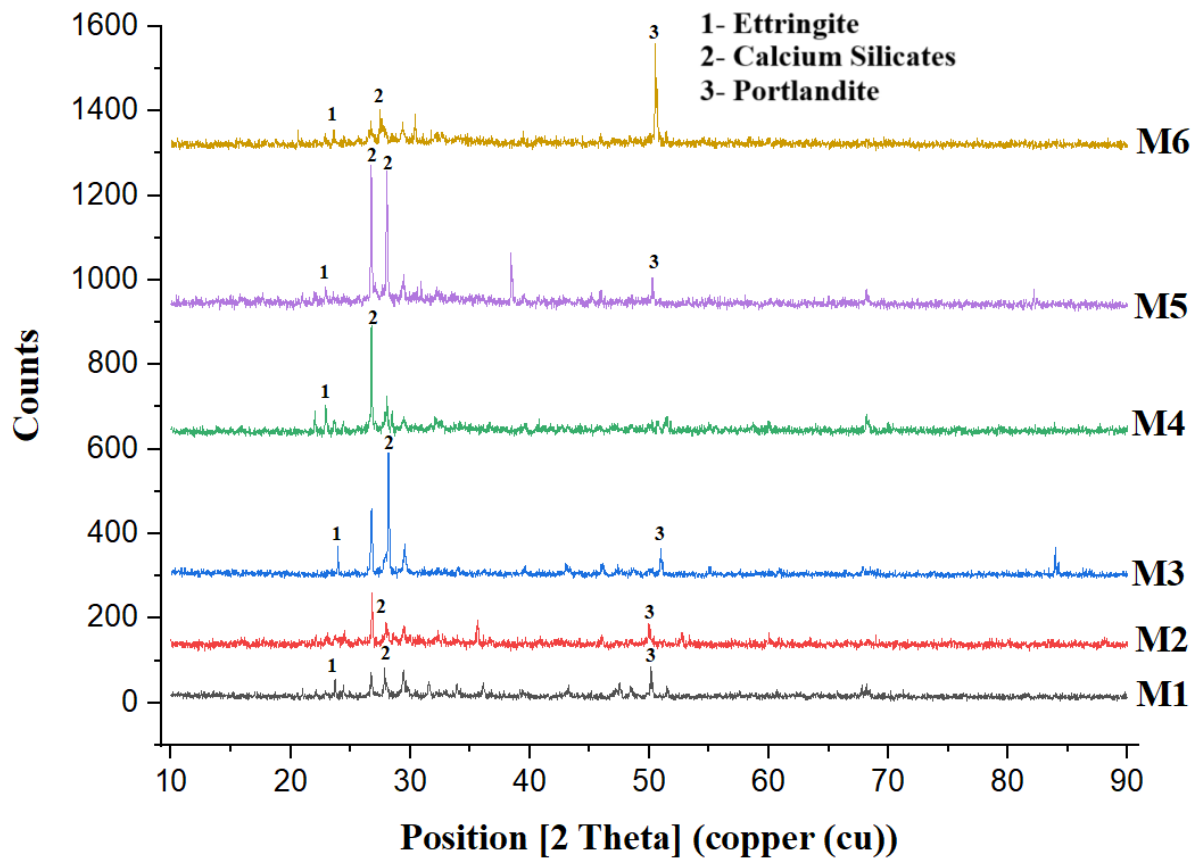
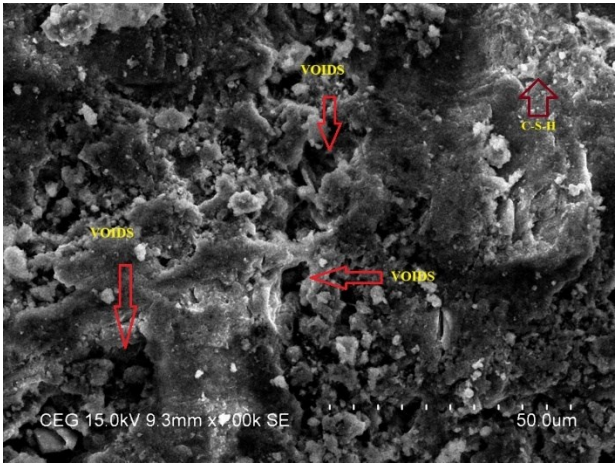


Figure 7. XRD analysis of concrete mixes incorporating jarosite-GGBS blends.

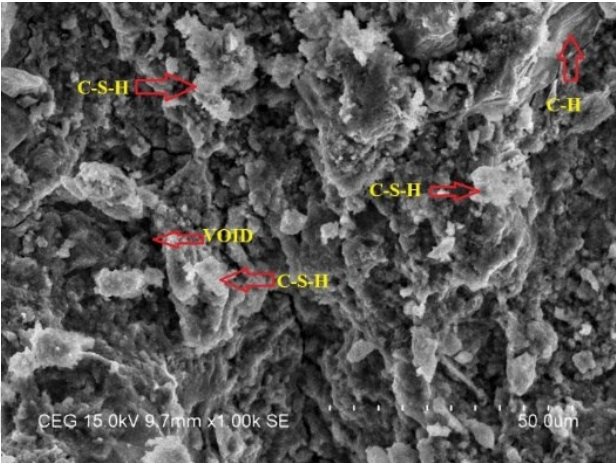
8. Scanning electron microscope analysis

A highly effective way to study the morphology of concrete-based composites is through scanning electron microscopy. The change in the concrete structure by incorporating GGBS and Jarosite is obtained for specimens M1 and M3 after 28 days of curing. The scanning electron microscope was taken at two levels of magnification, 1000 and 6000 times magnification. Figure 8. a and b represent the 1000-time magnification of specimens M1 and M3, respectively. Similarly, figure 8. c and d represent the 6000-time magnification of specimens M1 and M3, respectively. Vibrant white and black particles were identified as CSH gel and aggregates, respectively, according to the published literature (Yazici 2007). Figure 8 shows that the addition of jarosite has a dense microstructure, which justifies the lower concentration of the voids. The combination of GGBS and Jarosite provided a comparatively significant

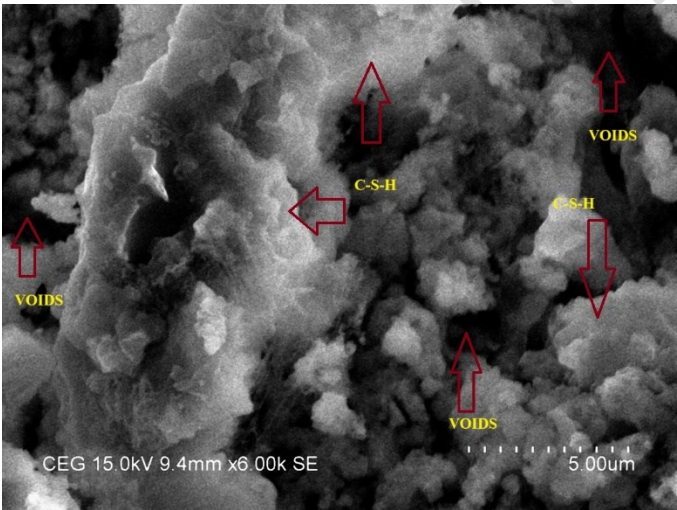
242 reduction in the ettringite formation (Saini et al. 2022a). The study depicts the formation of the massive
243 volume of needle-like structure identified as ettringite. These ettringite lead to lower compressive
244 strength and durability of the concrete. In this current study, Figure 8 proves deficient needle-like
245 formation; instead, a large CSH formation was identified. This reduced voids and ettringite formation
246 and visible formation of excess CSH and CH justifies the increase in strength properties.



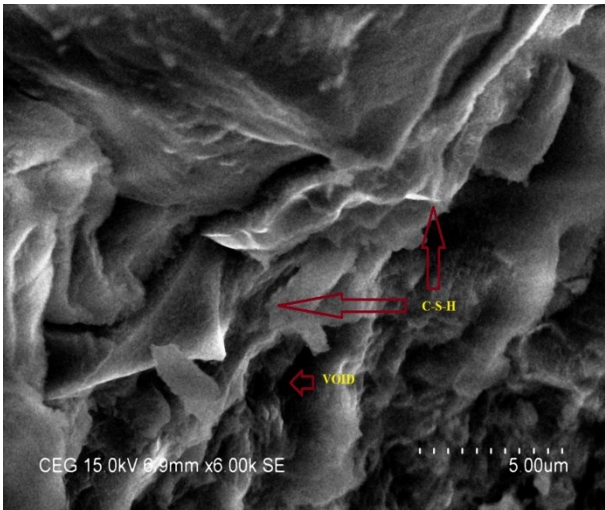
(a)



(b)



(c)



(d)

251 **Figure 8.** (a) Sem image of control concrete in 1000 magnification, (b) Sem image of M3 mix concrete
252 in 1000 magnification, (c) Sem image of control concrete in 6000 magnification, (d) Sem image of M3
253 mix concrete in 6000 magnification.

254 9. Conclusion

255 This study determined the impacts of GGBS and Jarosite on different concrete properties. The effect was
256 evaluated by replacing jarosite-GGBS blends for cement in a concrete mix and comparing the properties
257 to an M30 mix. The mechanical and microstructural properties (including the control mix) are
258 investigated by blending six different concrete mixes. The following conclusions are proposed:

- 259 • The addition of Jarosite with GGBS complimented the mechanical behavior of concrete for the
260 M3 mix with 20%GGBS and 10% Jarosite as a partial replacement of Ordinary Portland cement,
261 providing the optimum strength properties. The strength of the concrete mix containing jarosite
262 improved as the curing period was prolonged.
- 263 • The maximum increase in compressive strength is 50.93% higher than the conventional M30
264 concrete mix.
- 265 • The XRD analysis reveals that the silicate peaks are high at M3, M4, and M5 samples, supporting
266 the strength gain by replacing Jarosite and GGBS blends. The M6 peaks indicate a high
267 Portlandite, indicating a higher amount of unreacted cement content. This proves that the
268 replacement limit of jarosite with OPC cement concrete is 25%.
- 269 • The microstructural analysis by scanning electron microscope images revealed that the CSH gel
270 and CH gel formation in all the concrete mixes and the voids in the concrete decreased as the
271 jarosite replacement percentage increased. However, the cluster of CSH is observed to reduce
272 with a replacement level of 20% or higher, leading to a decrease in strength properties. The

addition of GGBS resulted in the reduction of needle-shaped ettringite formation, which affects the concrete strength properties.

As stated, jarosite is generated yearly in vast quantities, with a large percentage going to landfills. This raises deep concerns related to the environment. According to our scientific investigation, Jarosite-GGBS blended mix can be used as a supplementary cementitious material in concrete. The utilisation of jarosite in concrete provides a sustainable approach to the disposal of jarosite and reduces the consumption of Cement to a certain level.

10. Scope of future work.

The GGBS-Jarosite blends provided a higher increase in mechanical properties compared to the previous studies. In the future, properties such as acid attack resistance, rapid chloride penetration, and water absorption of the developed concrete must be studied.

References

- Agrawal A, Sahu KK, Pandey BD. Solid waste management in non-ferrous industries in India. *Resour. Conserv. Recycl.* 2004;42(2):99–120.
- Ainie Mat Dom A, Jamaluddin N, Azlina Abdul Hamid N, Siok Hoon C. A Review: GGBS as a Cement Replacement in Concrete. *IOP Conf. Ser. Earth Environ. Sci.* 2022;1022(1).
- Asokan P, Saxena M, Asolekar SR. Recycling hazardous jarosite waste using coal combustion residues. *Mater. Charact.* 2010;61(12):1342–55.
- Bumanis G, Vitola L, Stipniece L, Locs J, Korjamins A, Bajare D. Evaluation of Industrial by-products as pozzolans: A road map for use in concrete production. *Case Stud. Constr. Mater.* [Internet]. Elsevier Ltd.; 2020;13:e00424. Available from: <https://doi.org/10.1016/j.cscm.2020.e00424>
- Delbeke J, Runge-Metzger A, Slingenberg Y, Werksman J. The Paris agreement. *Toward a Clim. Eur. Curbing*

295 Trend. 2019.

296 Gupta C, Prasad A. Variables controlling strength of lime stabilized jarosite waste. *Int. J. Geo-Engineering*
 297 [Internet]. Springer Singapore; 2018a;9(1). Available from: <https://doi.org/10.1186/s40703-018-0074-2>

298 Gupta C, Prasad A. A parametric strength study of jarosite waste. *Proc. Inst. Civ. Eng. Waste Resour. Manag.*
 299 2018b;170(3+4):149–61.

300 Gupta C, Prasad A. Strength and Durability of Lime-Treated Jarosite Waste Exposed to Freeze and Thaw. *J.*
 301 *Cold Reg. Eng.* 2018c;32(1):1–11.

302 Gupta S, Chaudhary S. State of the art review on supplementary cementitious materials in India – II:
 303 Characteristics of SCMs, effect on concrete and environmental impact. *J. Clean. Prod.* [Internet]. Elsevier Ltd;
 304 2022;357(November 2021):131945. Available from: <https://doi.org/10.1016/j.jclepro.2022.131945>

305 Katsioti M, Tsakiridis PE, Agatzini-Leonardou S, Oustadakis P. Examination of the jarosite-alunite precipitate
 306 addition in the raw meal for the production of Portland and sulfoaluminate-based cement clinkers. *Int. J. Miner.*
 307 *Process.* 2005;76(4):217–24.

308 Khaiyum MZ, Sarker S, Kabir G. Evaluation of Carbon Emission Factors in the Cement Industry: An Emerging
 309 Economy Context. *Sustainability.* 2023;15(21):15407.

310 Khotbehsara MM, Mohseni E, Yazdi MA, Sarker P, Ranjbar MM. Effect of nano-CuO and fly ash on the
 311 properties of self-compacting mortar. *Constr. Build. Mater.* Elsevier Ltd; 2015;94:758–66.

312 Koushkbaghi M, Kazemi MJ, Mosavi H, Mohseni E. Acid resistance and durability properties of steel fiber-
 313 reinforced concrete incorporating rice husk ash and recycled aggregate. *Constr. Build. Mater.* [Internet]. Elsevier
 314 Ltd; 2019;202:266–75. Available from: <https://doi.org/10.1016/j.conbuildmat.2018.12.224>

315 Kumar S, Gupta RC, Thomas BS, Mehra P. Aggregate replacement and its usefulness in cement concrete for
 316 sustainable development—A study on rubber, Jarosite and sandstone aggregates. *Adv. Intell. Syst. Comput.*
 317 2016;493:13–25.

318 Mehra P, Gupta RC, Thomas BS. Assessment of durability characteristics of cement concrete containing jarosite.
 319 J. Clean. Prod. [Internet]. Elsevier Ltd; 2016a;119:59–65. Available from:
 320 <http://dx.doi.org/10.1016/j.jclepro.2016.01.055>

321 Mehra P, Gupta RC, Thomas BS. Properties of concrete containing jarosite as a partial substitute for fine
 322 aggregate. J. Clean. Prod. [Internet]. Elsevier Ltd; 2016b;120:241–8. Available from:
 323 <http://dx.doi.org/10.1016/j.jclepro.2016.01.015>

324 Mehra P, Kumar S, Thomas BS, Gupta RC. Analysis on the hazardous jarosite added concrete. Constr. Build.
 325 Mater. [Internet]. Elsevier Ltd; 2018;191:253–9. Available from:
 326 <https://doi.org/10.1016/j.conbuildmat.2018.10.006>

327 Mymrin A V, Ponte A H, Impinnisi R P. potential application of acid jarosite waste as the main component of
 328 construction materials.pdf. Constr. Build. Mater. 2005;19:141–6.

329 Naveen Arasu N, Natarajan M, Balasundaram N, Parthasaarathi R. Utilizing recycled nanomaterials as a partial
 330 replacement for cement to create high-performance concrete. Glob. Nest J. 2023;25(6):89–92.

331 Pappu A, Saxena M, Asolekar SR. Jarosite characteristics and its utilisation potentials. Sci. Total Environ.
 332 2006;359(1–3):232–43.

333 Pappu A, Saxena M, Asolekar SR. Solid wastes generation in India and their recycling potential in building
 334 materials. Build. Environ. 2007;42(6):2311–20.

335 Paramasivan S, Rajagopal T, Nadu T. Strength studies on concrete using e-palstic waste as coarse aggregate.
 336 Glob. NEST J. 2023;

337 Rakesh Kumar Reddy R, Yaragal SC, Sanjay VK. Processing of laboratory concrete demolition waste using ball
 338 mill. Mater. Today Proc. [Internet]. Elsevier Ltd; 2023; Available from:
 339 <https://doi.org/10.1016/j.matpr.2023.03.193>

340 Rashad AM. An investigation of high-volume fly ash concrete blended with slag subjected to elevated
 341 temperatures. J. Clean. Prod. [Internet]. Elsevier Ltd; 2015;93:47–55. Available from:

342 <http://dx.doi.org/10.1016/j.jclepro.2015.01.031>

343 Ray S, Daudi L, Yadav H, Ransinchung GD. Utilization of Jarosite waste for the development of sustainable
344 concrete by reducing the cement content. *J. Clean. Prod.* 2020;272.

345 Saini SK, Ransinchung GD, Kumar P. Effect of Different Mineral Admixtures on the Performance of Pavement
346 Quality Concrete Containing the Optimum Amount of Jarosite as Partial Replacement of Cement. *Arab. J. Sci.*
347 *Eng.* [Internet]. Springer Berlin Heidelberg; 2022a;47(10):13523–35. Available from:
348 <https://doi.org/10.1007/s13369-022-06892-5>

349 Saini SK, Ransinchung GD, Kumar P, Ray S. Investigation of jarosite-cement blends for hydration process and
350 mechanical behavior in PQC mixes. *Innov. Infrastruct. Solut.* [Internet]. Springer International Publishing;
351 2022b;7(3):1–13. Available from: <https://doi.org/10.1007/s41062-021-00707-6>

352 Sharma A, Gupta AK, Ganguly R. Impact of open dumping of municipal solid waste on soil properties in
353 mountainous region. *J. Rock Mech. Geotech. Eng.* [Internet]. Elsevier Ltd; 2018;10(4):725–39. Available from:
354 <https://doi.org/10.1016/j.jrmge.2017.12.009>

355 Siddique R. Utilization of industrial by-products in concrete. *Procedia Eng.* [Internet]. Elsevier B.V.;
356 2014;95(Scescm):335–47. Available from: <http://dx.doi.org/10.1016/j.proeng.2014.12.192>

357 Sunil Bhagwan Yamgar, S.R.Takkalaki. Study and Analysis of Strength of GGBS Concrete. *Int. J. Eng. Manag.*
358 *Res.* 2018;8(6):28–47.

359 Thirukumaran T, Krishnapriya S, Priya V, A SFB, Anandhalakshmi R, Dinesh S, et al. Utilizing rice husk ash as
360 a bio-waste material in geopolymer composites with aluminium oxide. *Glob. NEST J.* 2023;25(6):119–29.

361 V.mymrin, Vaamonde V. New Construction material from spanish jarosite. *Miner. Eng.* 1999;12(11):1399–402.

362 Wang F, Meng F, Feng T, Wang Y, Jiang J, Shi J. Effect of stone powder content on the mechanical properties
363 and microstructure of tunnel slag aggregate-based concrete. *Constr. Build. Mater.* [Internet]. Elsevier Ltd;
364 2023;388(April):131692. Available from: <https://doi.org/10.1016/j.conbuildmat.2023.131692>

365 Yazici H. Utilization of coal combustion byproducts in building blocks. *Fuel*. 2007;86(7–8):929–37.

366 Zhaurova M, Soukka R, Horttanainen M. Multi-criteria evaluation of CO2 utilization options for cement plants
367 using the example of Finland. *Int. J. Greenh. Gas Control* [Internet]. Elsevier Ltd; 2021;112(October):103481.
368 Available from: <https://doi.org/10.1016/j.ijggc.2021.103481>

369

ACCEPTED MANUSCRIPT